

# Differential Noise Figure and Gain De-Embedding: the Wave Approach

Janusz A. Dobrowolski

**Abstract**—The paper presents complete analysis of differential amplifier noise figure single-ended measurement setup. The analysis is based on scattering matrix representation for the network and wave representation for noise. As a result, there are presented equations allowing the differential amplifier gain and noise figure to be de-embedded with single-ended measurements. De-embedding equations are given for the balanced amplifier and for the fully differential amplifier.

**Keywords**—noise figure, differential noise figure, differential noise figure de-embedding

## I. INTRODUCTION

TODAY most of the RF and microwave electronic circuits realized as RFICs or MMICs use differential topologies [1]. Front-end low noise amplifiers are fully differential. Measurements of gain and noise figure of such circuits require differential signal excitation at the input and differential signal measurements at the output. Because standard microwave instruments such as network analyzers or noise figure meters are single ended they are adopted for differential amplifier measurements by application of two baluns, one balun inserted before the differential input and one balun inserted at the differential output of the device under test (DUT) [6,7,8,9,10,11]. In such configuration of single ended measurement set it is necessary to take into account losses and noise introduced to the system by two baluns surrounding the DUT. This paper presents the solution equations of the differential noise figure de-embedding with only single-ended noise measurements. De-embedding equations are derived for two types of differential amplifiers, balanced amplifier and fully differential amplifier. Derivation of de-embedding equations is based on the scattering parameters description for networks and the noise wave representation for noise [2,3,4].

## II. NOISE FIGURE OF BALANCED AMPLIFIER IN SINGLE-ENDED ENVIRONMENT

Today's microwave noise figure measuring instruments provide only a single-ended input noise and measure the single-ended output noise. Such instruments are converted to differential by inserting a 3 dB/180° power divider (a balun) before the input of a differential device under test (DDUT),

The author is with the Institute of Electronic Systems, Faculty of Electronics and Information Technology, Warsaw University of Technology, Nowowiejska 15/19, 00-665 Warsaw, Poland (e-mail: jad@ise.pw.eu.pl).

and a 3 dB/180° power combiner (a balun) at the output of the DDUT. Fig. 1 illustrates such measurement arrangement.

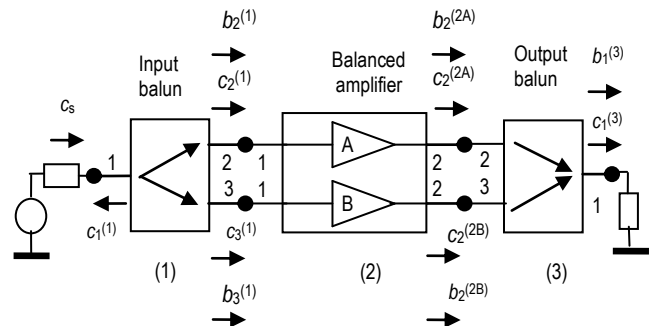


Fig. 1. Noise waves at ports of a balanced/differential amplifier in the single-ended environment.

Passive baluns used as the single-ended to differential signal converters are bidirectional and matched. They split the input signal at port 1 equally into ports 2 and 3, but as the anti-phase waves. When any two ports of the balun are loaded by the reference impedances, usually 50 Ω, the input impedance of the third port is also 50 Ω. The scattering matrix of the matched balun equals

$$\mathbf{S} = \begin{bmatrix} 0 & S_{12} & -S_{12} \\ S_{21} & 0 & S_{23} \\ -S_{21} & S_{23} & 0 \end{bmatrix} \quad (1)$$

The network presented in Fig. 1 is the cascade connection of three multiport networks, numbered 1, 2, and 3. For the input balun, network 1, its output noise waves are

$$b_2^{(1)} = c_2^{(1)} + S_{21}^{(1)} c_s \quad (2)$$

$$b_3^{(1)} = c_3^{(1)} - S_{21}^{(1)} c_s \quad (3)$$

For the balanced amplifier, network 2

$$b_2^{(2A)} = c_2^{(2A)} + S_{21}^{(2A)} a_1^{(2A)} = c_2^{(2A)} + S_{21}^{(2A)} b_2^{(1)} \quad (4)$$

$$b_2^{(2B)} = c_2^{(2B)} + S_{21}^{(2B)} a_1^{(2B)} = c_2^{(2B)} + S_{21}^{(2B)} b_3^{(1)} \quad (5)$$

For the output balun, network 3, we can write

$$b_1^{(3)} = c_1^{(3)} + S_{13}^{(3)} a_2^{(3)} - S_{13}^{(3)} a_3^{(3)} = c_1^{(3)} + S_{13}^{(3)} b_2^{(2A)} - S_{13}^{(3)} b_2^{(2B)} \quad (6)$$

Inserting (2) through (5) into (6), we get

$$b_1^{(3)} = c_1^{(3)} + S_{13}^{(3)}(c_2^{(2A)} - c_2^{(2B)}) + S_{13}^{(3)}S_{21}^{(2)}(c_2^{(1)} - c_3^{(1)}) + 2S_{21}^{(1)}S_{21}^{(2)}S_{13}^{(3)}c_s \quad (7)$$

In (2) through (7)  $c$  are amplitudes of noise waves representing internal noise sources in networks while  $b$  are amplitudes of outgoing noise waves at network ports.

Using (7), we can write the total noise power density at the output of the cascade as

$$\begin{aligned} \overline{|b_1^{(3)}|^2} &= \overline{|c_1^{(3)}|^2} + |S_{13}^{(3)}|^2 \left( \overline{|c_2^{(2A)}|^2} + \overline{|c_2^{(2B)}|^2} \right) \\ &+ |S_{13}^{(3)}|^2 |S_{21}^{(2)}|^2 \left( \overline{|c_2^{(1)}|^2} + \overline{|c_3^{(1)}|^2} - 2\text{Re}\{c_2^{(1)}c_3^{(1)*}\} \right) \\ &+ 4|S_{21}^{(1)}|^2 |S_{21}^{(2)}|^2 |S_{13}^{(3)}|^2 \overline{|c_s|^2} \end{aligned} \quad (8)$$

or

$$\begin{aligned} \overline{|b_1^{(3)}|^2} &= \overline{|c_1^{(3)}|^2} + 2G^{(3)} \overline{|c_2^{(2)}|^2} \\ &+ 2G^{(2)}G^{(3)} \left( \overline{|c_2^{(1)}|^2} - \text{Re}\{c_2^{(1)}c_3^{(1)*}\} \right) \\ &+ 4kTG^{(1)}G^{(2)}G^{(3)} \end{aligned} \quad (9)$$

where

$$G^{(1)} = |S_{21}^{(1)}|^2, G^{(2)} = |S_{21}^{(2)}|^2, G^{(3)} = |S_{13}^{(3)}|^2 \text{ and } \overline{|c_s|^2} = kT.$$

It is assumed in (9) that the noise generated in the single ended amplifiers is not correlated.

#### A. Noise Figure of the Input Balun in Single Ended Configuration

For presented in Fig. 2 network 1, considered between port 1 and port 2 as a single-ended two-port network, we can write

$$\overline{|b_2|^2} = \overline{|c_2^{(1)}|^2} + |S_{23}^{(1)}|^2 \overline{|c_a|^2} + |S_{21}^{(1)}|^2 \overline{|c_s|^2} \quad (10)$$

In (10), noise wave  $c_a$  represents the thermal noise generated by the matched load at port 3 of the balun.

In further consideration we consider noise figure for a two-port defined as

$$F = \frac{\text{Available power of total noise at output port}}{\text{Available power of noise due to source resistor alone}} \quad (11)$$

According to (11) the noise figure of considered network equals

$$\begin{aligned} F^{(1)} &= \frac{\overline{|b_2|^2}}{|S_{21}^{(1)}|^2 \overline{|c_s|^2}} = \frac{\overline{|c_2^{(1)}|^2} + |S_{23}^{(1)}|^2 \overline{|c_a|^2} + |S_{21}^{(1)}|^2 \overline{|c_s|^2}}{|S_{21}^{(1)}|^2 \overline{|c_s|^2}} \\ &= \frac{\overline{|c_2^{(1)}|^2} + kT|S_{23}^{(1)}|^2 + kT_0|S_{21}^{(1)}|^2}{kT_0|S_{21}^{(1)}|^2} \end{aligned} \quad (12)$$

where  $T$  is the physical temperature of the matched load of port 3 of the balun, and  $T_0 = 290$  K is the standard reference temperature of the signal source.

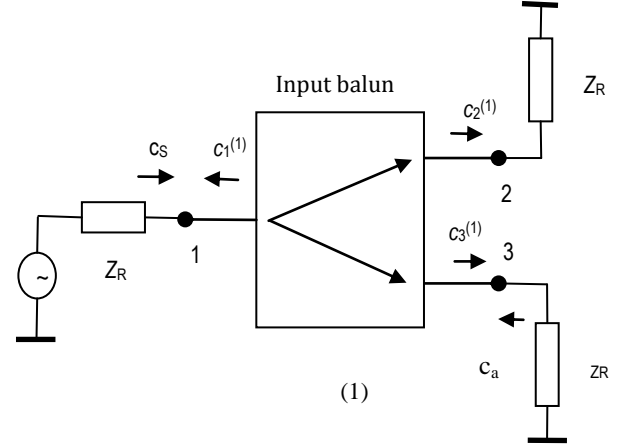


Fig. 2. Network 1, the input balun in the single-ended configuration with the equivalent noise wave sources at its ports.

For a balun with high isolation between output ports, we can assume that  $S_{23} = S_{32} = 0$ . In such case, we have

$$F^{(1)} = \frac{\overline{|c_2^{(1)}|^2} + kT_0|S_{21}^{(1)}|^2}{kT_0|S_{21}^{(1)}|^2} = \frac{\overline{|c_2^{(1)}|^2} + kT_0G^{(1)}}{kT_0G^{(1)}} = 1 + \frac{\overline{|c_2^{(1)}|^2}}{kT_0G^{(1)}} \quad (13)$$

where  $G^{(1)} = |S_{21}^{(1)}|^2$ , and  $T_0 = 290$  K.

#### B. Noise Figure of the Output Balun in Single-Ended Configuration

Figure 3 illustrates the single-ended configuration of the output balun. This balun is considered, between port 2 and port 1, as the two-port network 3.

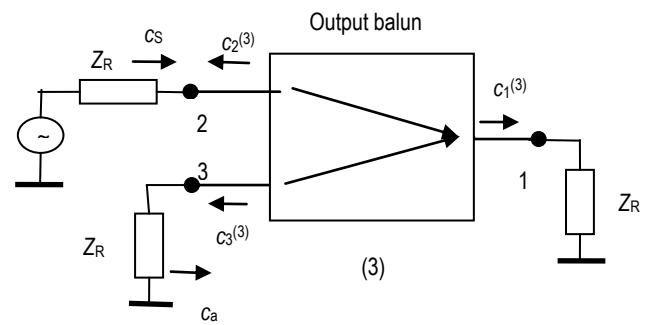


Fig. 3. Network 3, the output balun in single-ended configuration with equivalent noise wave sources at its ports.

For the output balun working as a power combiner, we have

$$\overline{|b_1|^2} = \overline{|c_1^{(3)}|^2} + |S_{13}^{(3)}|^2 \overline{|c_a|^2} + |S_{12}^{(3)}|^2 \overline{|c_s|^2} \quad (14)$$

In (14),  $c_1$  represents the thermal noise generated by the balun,  $c_a$  represents the thermal noise generated by the matched load of port 3 of the balun, and  $c_s$  corresponds to the

thermal noise of the internal impedance of the single-ended signal source connected to port 2 of the balun.

The noise figure of this network

$$F^{(3)} = \frac{\overline{|b_1|}^2}{\overline{|S_{12}^{(3)}|^2 |c_s|}^2} = \frac{\overline{|c_1^{(3)}|^2} + \overline{|S_{13}^{(3)}|^2 |c_a|^2} + \overline{|S_{12}^{(3)}|^2 |c_s|^2}}{\overline{|S_{12}^{(3)}|^2 |c_s|^2}} \quad (15)$$

$$= \frac{\overline{|c_1^{(3)}|^2} + kT |S_{13}^{(3)}|^2 + kT_0 |S_{12}^{(3)}|^2}{kT_0 |S_{12}^{(3)}|^2}$$

Assuming that the physical temperature  $T$  of the balun equals the standard reference temperature  $T_0$ , that is  $T = T_0 =$

290 K, we have  $\overline{|c_s|}^2 = \overline{|c_a|}^2 = kT_0$ , and

$$\overline{|b_1|}^2 = \overline{|c_1^{(3)}|^2} + kT_0 |S_{13}^{(3)}|^2 + kT_0 |S_{12}^{(3)}|^2 \quad (16)$$

Assuming that  $|S_{13}^{(3)}|^2 = |S_{12}^{(3)}|^2$ , the noise figure of this network

$$F^{(3)} = \frac{\overline{|c_1^{(3)}|^2} + 2kT_0 |S_{12}^{(3)}|^2}{kT_0 |S_{12}^{(3)}|^2} = \frac{\overline{|c_1^{(3)}|^2} + 2kT_0 G^{(3)}}{kT_0 G^{(3)}} = 2 + \frac{\overline{|c_1^{(3)}|^2}}{kT_0 G^{(3)}} \quad (17)$$

where  $G^{(3)} = |S_{12}^{(3)}|^2$ .

### C. Noise Figure of Balanced Amplifier

We will derive now the noise figure of the differential amplifier, the network 2, in the cascade presented in Fig. 1. Because the total noise power density at the output of the single-ended amplifier comprising the differential amplifier is

$$\overline{|b_2|}^2 = \overline{|c_2^{(2)}|^2} + \overline{|S_{21}^{(2)}|^2 |c_s|^2} \quad (18)$$

than the noise figure of the single-ended amplifier equals

$$F^{(2)} = \frac{\overline{|c_2^{(2)}|^2} + kT_0 |S_{21}^{(2)}|^2}{kT_0 |S_{21}^{(2)}|^2} = 1 + \frac{\overline{|c_2^{(2)}|^2}}{kT_0 G^{(2)}} \quad (19)$$

where  $G^{(2)} = |S_{21}^{(2)}|^2$ .

Now we are able to derive the total noise figure  $F^{(\text{TOT})}$  of the cascade network as a function of the individual noise figures  $F^{(1)}$ ,  $F^{(2)}$  and  $F^{(3)}$  and the individual power gains  $G^{(1)}$ ,  $G^{(2)}$  and  $G^{(3)}$  of networks, configuring the network presented in Fig. 1.

Because the network 1 is passive and its noise wave correlation matrix satisfies the equation [5]

$$\mathbf{C}_S = kT(\mathbf{I} - \mathbf{S}\mathbf{S}^+) \quad (20)$$

we can derive from (28) that

$$\text{Re}\{c_2^{(1)} c_3^{(1)*}\} = kT \left( |S_{21}^{(1)}|^2 - 2\text{Re}\{S_{22}^{(1)} S_{23}^{(1)*}\} \right) \quad (21)$$

Using relations (8), (13), (17), (19) and (21), we receive the total noise power density at the output of the cascade as

$$\overline{|b_1^{(3)}|^2} = kT_0 (F^{(3)} - 2)G^{(3)} + 2kT_0 (F^{(2)} - 1)G^{(2)}G^{(3)} + 2G^{(2)}G^{(3)} \left[ kT_0 G^{(1)} \left( F^{(1)} - 1 - \frac{|S_{23}^{(1)}|^2}{G^{(1)}} \right) - kT_0 \left( |S_{21}^{(1)}|^2 - 2\text{Re}\{S_{22}^{(1)} S_{23}^{(1)*}\} \right) \right] + 4kT_0 G^{(1)}G^{(2)}G^{(3)} \quad (22)$$

The output noise power density related to the thermal noise generated by the signal source resistance alone

$$\overline{|b_{is}^{(3)}|^2} = 4kT_0 G^{(1)}G^{(2)}G^{(3)} \quad (23)$$

while the available power gain of the cascade is

$$G^{(\text{TOT})} = 4G^{(1)}G^{(2)}G^{(3)} \quad (24)$$

When we assume ideal isolation between ports 2 and 3 of the input balun, what means that  $S_{23}^{(1)} = S_{32}^{(1)} = 0$ , we have

$$\overline{|b_1^{(3)}|^2} = kT_0 (F^{(3)} - 2)G^{(3)} + 2kT_0 (F^{(2)} - 1)G^{(2)}G^{(3)} + 2kT_0 (F^{(1)} - 2)G^{(1)}G^{(2)}G^{(3)} + 4kT_0 G^{(1)}G^{(2)}G^{(3)} \quad (25)$$

In accordance with the noise figure definition given by (11), the noise figure of the cascade network presented in Fig. 4 equals

$$F^{(\text{TOT})} = \frac{\left[ kT_0 (F^{(3)} - 2)G^{(3)} + 2kT_0 (F^{(2)} - 1)G^{(2)}G^{(3)} + 2kT_0 F^{(1)}G^{(1)}G^{(2)}G^{(3)} \right]}{4kT_0 G^{(1)}G^{(2)}G^{(3)}} = \frac{F^{(1)}}{2} + \frac{F^{(2)} - 1}{2G^{(1)}} + \frac{F^{(3)} - 2}{4G^{(1)}G^{(2)}} \quad (26)$$

Recall that  $G^{(1)}$  and  $G^{(3)}$  are single-ended gains of the baluns and  $F^{(1)}$  and  $F^{(3)}$  are single-ended noise figures of the baluns. Similarly  $G^{(\text{TOT})}$  and  $F^{(\text{TOT})}$  are single-ended gain and single ended noise figure of the cascade which are measured simultaneously by single-ended noise figure meter. The two unknowns in (24) and in (26) are  $F^{(2)}$  and  $G^{(2)}$ . Using (24) and (26), the balanced amplifier gain  $G^{(2)}$  and the noise figure  $F^{(2)}$  may be accurately de-embedded on the basis of single-ended measurements of the cascade and of the baluns. These equations are identical with a relations derived and presented in [8].

It is recommended yet to derive relation between  $F^{(2)}$  and the differential noise figure of the balanced amplifier. Because

the differential-mode noise wave at the output of the balanced amplifier

$$b_{d2} = \frac{b_2^{(2A)} - b_2^{(2B)}}{\sqrt{2}} = \frac{1}{\sqrt{2}} \left( c_2^{(2A)} - c_2^{(2B)} + S_{21}^{(2A)} c_{s1} - S_{21}^{(2B)} c_{s2} \right) \quad (27)$$

than the power density of the differential-mode output noise represented by  $b_{d2}$  is

$$\overline{|b_{d2}|^2} = \frac{1}{2} \left( \overline{|c_2^{(2A)}|^2} + \overline{|c_2^{(2B)}|^2} + kT_0 \left( |S_{21}^{(2A)}|^2 + |S_{21}^{(2B)}|^2 \right) \right) \quad (28)$$

because  $\overline{|c_{s1}|^2} = \overline{|c_{s2}|^2} = kT_0$ ,  $T_0 = 290$  K.

According to the definition of the noise figure given by (11), the noise figure of the differential amplifier

$$F_d = \frac{\overline{|c_2^{(2A)}|^2} + \overline{|c_2^{(2B)}|^2} + kT_0 \left( |S_{21}^{(2A)}|^2 + |S_{21}^{(2B)}|^2 \right)}{kT_0 \left( |S_{21}^{(2A)}|^2 + |S_{21}^{(2B)}|^2 \right)} = 1 + \frac{\overline{|c_2^{(2A)}|^2} + \overline{|c_2^{(2B)}|^2}}{kT_0 \left( |S_{21}^{(2A)}|^2 + |S_{21}^{(2B)}|^2 \right)} \quad (29)$$

where  $T_0 = 290$  K.

Because the noise figures of the single-ended amplifiers are

$$F^{(A)} = \frac{\overline{|c_2^{(2A)}|^2} + kT_0 |S_{21}^{(2A)}|^2}{kT_0 |S_{21}^{(2A)}|^2} = \frac{\overline{|c_2^{(2A)}|^2} + kT_0 G^{(A)}}{kT_0 G^{(A)}} \quad (30)$$

and

$$F^{(B)} = \frac{\overline{|c_2^{(2B)}|^2} + kT_0 |S_{21}^{(2B)}|^2}{kT_0 |S_{21}^{(2B)}|^2} = \frac{\overline{|c_2^{(2B)}|^2} + kT_0 G^{(B)}}{kT_0 G^{(B)}} \quad (31)$$

than substituting (30) and (31) into (29), we get

$$F_d = 1 + \frac{G^{(A)}(F^{(A)} - 1) + G^{(B)}(F^{(B)} - 1)}{G^{(A)} + G^{(B)}} \quad (32)$$

In (30) through (32),  $G^{(A)} = |S_{21}^{(2A)}|^2$  and  $G^{(B)} = |S_{21}^{(2B)}|^2$  are, respectively, power gains of the amplifier A and the amplifier B.

When  $G^{(A)} = G^{(B)} = G$

$$F_d = \frac{F^{(A)} + F^{(B)}}{2} \quad (33)$$

and for  $F^{(A)} = F^{(B)} = F$

$$F_d = F \quad (34)$$

This proves that a balanced amplifier that comprises two identical single-ended amplifiers has the same noise figure as each of the constituent single-ended amplifiers. This result comes from the fact that the noise of two amplifiers A and B is not correlated.

### III. NOISE FIGURE OF DIFFERENTIAL AMPLIFIER IN SINGLE-ENDED ENVIRONMENT

Figure 4 illustrates fully differential amplifier excited by differential signal source.

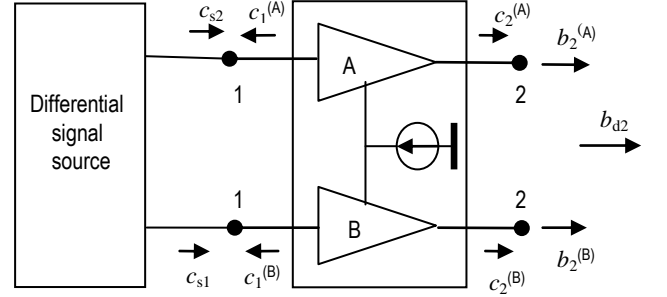


Fig. 4. Differential amplifier excited by differential signal source

Because the total power density of the output differential noise is

$$\overline{|b_{d2}|^2} = \frac{\overline{|b_3^{(2)} - b_4^{(2)}|^2}}{2} = \overline{|c_3^{(2)}|^2} + \overline{|c_4^{(2)}|^2} - \overline{c_3^{(2)} c_4^{(2)*}} - \overline{c_3^{(2)*} c_4^{(2)}} + |S_{31}^{(2)} - S_{41}^{(2)}|^2 \overline{|c_{s1}|^2} + |S_{32}^{(2)} - S_{42}^{(2)}|^2 \overline{|c_{s2}|^2} \quad (35)$$

then applying  $S_{32} = S_{41} = A/2$ ,  $S_{31} = S_{42} = -A/2$  and assuming that  $\overline{|c_{s1}|^2} = \overline{|c_{s2}|^2} = kT_0$ , the noise figure of the differential amplifier is

$$F = 1 + \frac{\overline{|c_3^{(2)}|^2} + \overline{|c_4^{(2)}|^2} - 2\text{Re}\{\overline{c_3^{(2)} c_4^{(2)*}}\}}{2kT_0 |A|^2} \quad (36)$$

For the cascade presented in Fig. 1 with fully differential amplifier as a second stage, the total noise power density at the output is

$$\overline{|b_1^{(3)}|^2} = \overline{|c_1^{(3)}|^2} + |S_{13}^{(3)}|^2 \left( \overline{|c_2^{(1)}|^2} + \overline{|c_2^{(2)}|^2} - 2\text{Re}\{\overline{c_3^{(2)} c_4^{(2)*}}\} \right) + |S_{13}^{(3)}|^2 \left( |S_{32}^{(2)} - S_{42}^{(2)}|^2 \overline{|c_2^{(1)}|^2} + |S_{31}^{(2)} - S_{41}^{(2)}|^2 \overline{|c_3^{(1)}|^2} + 2\text{Re}\{(S_{32}^{(2)} - S_{42}^{(2)})(S_{31}^{(2)} - S_{41}^{(2)}) \overline{c_2^{(1)} c_3^{(1)*}}\} \right) + |S_{21}^{(1)}|^2 |S_{32}^{(2)} - S_{31}^{(2)} + S_{41}^{(2)} - S_{42}^{(2)}|^2 |S_{13}^{(3)}|^2 \overline{|c_s|^2} \quad (37)$$

or

$$\begin{aligned} \overline{|b_1^{(3)}|^2} &= \overline{|c_1^{(3)}|^2} + G^{(3)} \left( \overline{|c_3^{(2)}|^2} + \overline{|c_4^{(2)}|^2} - 2\text{Re}\{c_3^{(2)}c_4^{(2)*}\} \right) \\ &+ G^{(2)}G^{(3)} \left( \overline{|c_2^{(1)}|^2} + \overline{|c_3^{(1)}|^2} - 2\text{Re}\{c_2^{(1)}c_3^{(1)*}\} \right) \\ &+ 4kT_0G^{(1)}G^{(2)}G^{(3)} \end{aligned} \quad (38)$$

where

$$G^{(1)} = |S_{21}^{(1)}|^2, G^{(2)} = |A|^2, G^{(3)} = |S_{13}^{(3)}|^2 \text{ and } \overline{|c_s|^2} = kT_0.$$

Using (35), (36), and (38) we can write

$$\begin{aligned} \overline{|b_1^{(3)}|^2} &= kT_0(F^{(3)} - 2)G^{(3)} + 2kT_0(F_d^{(2)} - 1)G^{(2)}G^{(3)} \\ &+ 2kT_0G^{(1)}G^{(2)}G^{(3)}F^{(1)} + 4kT_0G^{(1)}G^{(2)}G^{(3)} \end{aligned} \quad (39)$$

and finally

$$F^{(\text{TOT})} = 1 + \frac{F^{(1)}}{2} + \frac{F_d^{(2)} - 1}{2G^{(1)}} + \frac{F^{(3)} - 2}{4G^{(1)}G_d^{(2)}} \quad (40)$$

Because the output noise density due to the resistance of the signal source is

$$\overline{|b_1^{(3)}|^2} = 4kT_0G^{(1)}G_d^{(2)}G^{(3)} \quad (41)$$

the available power gain of the cascade

$$G^{(\text{TOT})} = 4G^{(1)}G_d^{(2)}G^{(3)} \quad (42)$$

In (40) and (42) all gains and noise figures, except  $G_d^{(2)}$  and  $F_d^{(2)}$ , are single ended quantities.  $G^{(1)}$  and  $G^{(3)}$  are single-ended gains of the baluns and  $F^{(1)}$  and  $F^{(3)}$  are single-ended noise figures of the baluns. Similarly,  $G^{(\text{TOT})}$  and  $F^{(\text{TOT})}$  are single-ended gain and single ended noise figure of the cascade which are measured simultaneously by single-ended noise figure meter. The two unknowns in (40) and in (42) are  $F_d^{(2)}$  and  $G_d^{(2)}$ . Using (40) and (42), the differential amplifier gain and the noise figure may be accurately de-embedded on the basis of single-ended measurements of the cascade and of the baluns.

## IV. CONCLUSION

Application of conventional, commercial single ended measurement equipment to characterize differential amplifiers requires location of two baluns at the input and at the output of a differential DUT. In consequence, the effect of the baluns should be taken into account and properly eliminated. This paper presents a complete analysis of such measurement setup and derivation of the noise figure formulas for a cascade of two-ports, three-ports such as baluns and differential four-ports.. From these formulas it is possible to extract the differential noise figure and gain of the differential amplifier. The derived formulas (26) and (40) allow exact de-embedding of a balanced amplifier and of a fully differential amplifier from balunes and other network elements required to measure their noise figure in single-ended measurement equipment.

## REFERENCES

- [1] D. E. Bockelman, and W. R. Eisenstadt, "Combined Differential and Common Mode Scattering Parameters: Theory and Simulation", *IEEE Trans. Microwave Theory and Techniques*, Vol. 43, No. 7, July 1997, pp. 1530-1539.
- [2] A. Ferrero, and M. Pirola, "Generalized Mixed-Mode S-Parameters", *IEEE Trans. Microwave Theory Techn.*, Vol. 54, No.1, January 2006, pp. 458-463.
- [3] P. B. Marks, and D. F. Williams, "A General Waveguide Circuit Theory", *Journal of Research of the National Institute of Standards and Technology*, vol. 97, 1992, pp. 533- 562.
- [4] S. W. Wedge, and D.B. Rutledge, "Noise Waves and Passive Linear Multiports", *IEEE Microwave and Guided Wave Letters*, Vol. 1, No. 5, May 1991, pp. 117-110.
- [5] H. Bosma, "On the Theory of Linear Noisy Systems", *Philips Research Reports*, Suppl., No. 10, 1967.
- [6] L. Belostotski, and J. W. Haslett, "A Technique for Differential Noise Figure Measurement of Differential LNAs", *IEEE Trans. Microwave Theory Techn.*, Vol. 57, No. 7, July 2008, pp. 1298- 1303.
- [7] L. F. Tiemeijer, R. M. T. Pijper, and E. van der Heiden, "Complete On-Wafer Noise-Figure Characterization of 60 GHz Differential Amplifier", *IEEE Trans. Microwave Theory Techn.*, Vol. 58, No. 6, June 2010, pp. 1599-1608.
- [8] A. A. Abidi, and J.C. Leete, "De-Embedding Noise Figure of Differential Amplifiers", *IEEE Journal of Solid State Circuits*, Vol. 34, No. 6, June 1999, pp. 882-885.
- [9] M. R. Robens, R. Wunderlich, and S. Heinen, "Differential Noise Figure De-Embedding: A Comparison of Available Approaches", *IEEE Trans. Microwave Theory Techn.*, Vol. 59, No. 5, May 2011, pp. 1397-1407.
- [10] O. Garcia-Perez, V. Gonzalez-Posadas, L. E. Garcia-Munioz, and D. Segovia-Vargas, "Noise Figure Measurement of Differential Amplifiers Using Nonideal Baluns", *IEEE Trans. Microwave Theory Techn.*, Vol. 59, No. 6, June 2011, pp. 1659-1664.
- [11] J. Dunsmore, S. Wood, "Vector Corrected Noise Figure and Noise Parameter Measurements of Differential Amplifiers", *Proc. 39<sup>th</sup> European Microwave Conference*, 29 Sept. – 1 Oct. 2009, Rome, Italy, pp. 707-710.